Macromolecules

pubs.acs.org/Macromolecules Article

Stearic Acid-Infused PDMS PolyMIPEs Exhibiting Shape Memory Behavior

Anthony Smith, Anna Brown, Jack Newman, and Neil Ayres*

Cite This: *Macromolecules* 2024, 57, 6796−6804 Read Online

ACCESS | Metrics & More | Article Recommendations | Supporting Information

ABSTRACT: Emulsion-templated polymerizations are an attractive route to prepare porous materials that possess broad tunability by controlling the features of the emulsion template. Emulsion-templated polymer materials possessing shape memory behavior have also been reported, usually using (meth)acrylate monomers. However, achieving shape memory properties in emulsion-templated materials with polymers that do not possess accessible thermal transitions, including polydimethylsiloxane (PDMS), remains challenging. Here, porous PDMS materials have been prepared with stearic acid within the continuous phase of the emulsion template. The inclusion of stearic acid imparts the material with a transition temperature of ∼70 °C, and the porous materials in this work obtained fixity >90% and recovery >95% over multiple shape memory cycles. These results demonstrate how low glass-transition temperature emulsion-templated polymer materials can easily be given shape memory properties. This work should be a starting point for studies of elastomeric emulsion-templated polymer materials in applications, including in soft robotics.

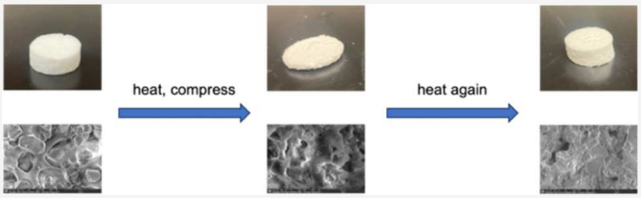

INTRODUCTION

Shape memory polymers[1] (SMPs) are a type of stimuli-responsive smart material[2−5] where temporary shapes can be programmed or "fixed" through network immobilization and the initial shape recovered upon exposure to a stimulus. SMPs have been used in a variety of applications, including for wire insulating, pipe corrosion resistance, biomedical devices, and artificial muscles.[6−10] Examples of stimuli that have been studied include heat,[11,12] electricity,[13] and pH.[14] When heat is used as a stimulus, SMPs are called thermoresponsive shape memory polymers.[15] Thermoresponsive SMPs use a material's thermal transition temperature (T_{trans}) as the temperature at which a material will undergo deformation and fixation or recover to the original shape. Fixing a thermoresponsive SMP into its temporary shape requires heating the material above its T_{trans}, deforming the material into a temporary shape, then cooling the SMP under deformation to "lock in" the temporary shape. The material in the temporary shape can be reheated above the transition temperature again to return to its initial processed shape.[16,17] For example, Liu and co-workers[18] designed a nanocomposite shape memory polymer from polycaprolactone, polyethylene glycol, and cellulose nanocrystals. The materials exhibited shape memory properties when heated past 37 °C, making them suitable candidates for surgical devices or self-tightening sutures that respond when subjected to the body's physiological conditions.

Porous polymer materials can be designed to possess advantageous properties including compressibility[19−21] and elasticity,[22−24] which when combined with their internal porosity enable these materials to be used in applications such as acoustic waveguiding,[25−27] size/chemical exclusion filtration,[28] and cell proliferation.[29] One method to synthesize porous polymers is through using an emulsion templating approach.[30] With this route, monomers are dissolved into a continuous phase that is immiscible with the dispersed phase of the emulsion template. The monomer in the continuous phase of the emulsion is polymerized, and the dispersed phase is removed resulting in a porous network. Polymerized high internal phase emulsions (PolyHIPEs) are a class of porous polymer that are polymerized from an emulsion template where the internal phase of the emulsion constitutes more than 74% of the volume fraction.[31] Formally, a medium internal phase emulsion (MIPE) has an internal volume fraction of 24−74%, while a low internal phase emulsion (LIPE) possesses less than 24% volume fraction of the dispersed phase.[32]

Shape memory behavior has also been reported in several porous polymer materials.[33−36] For example, Silverstein's group[37] introduced polyHIPEs with shape memory properties prepared from acrylate and methacrylate monomers bearing long crystallizable side chains, where the T_{trans} could be tuned by modifying the chain lengths on the monomers. An example of porous poly(ethylene glycol)-poly(caprolactone)-polydimethylsiloxane (PDMS) urethane materials possessing shape memory properties was reported by Ang et al.[38] These

Received: February 27, 2024
Revised: June 25, 2024
Accepted: June 27, 2024
Published: July 12, 2024

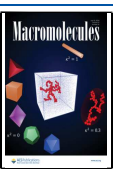

https://doi.org/10.1021/acs.macromol.4c00457
Macromolecules 2024, 57, 6796−6804

materials were not thermoresponsive but could respond to solvation in water due to the crystallization of poly(caprolactone) segments achieving recovery values of ∼25 to 60%. However, these materials were prepared through electrospinning and not emulsion templating. Polydimethylsiloxane has become ubiquitous in material chemistry applications due to its ideal material properties such as good thermal stability,[39] optical transparency,[40] and high flexibility.[41]

Several groups have introduced shape memory polymers that incorporate PDMS as a soft segment in their design owing to its relatively low glass-transition temperature.[42−45] For example, the Craig group[46] synthesized SMPs from a PDMS/spiropyran network, which provided covalent bond activation coupled with macroscopic reversibility. These materials were flexible and changed color in response to stress. To the best of our knowledge, there are no examples of a homopolymer network made from PDMS capable of shape memory behavior due to the lack of a switchable hard-segment or functional groups for network immobilization. Thus, preparing porous shape memory PDMS as the only polymer remains a challenge.

Herein, we were inspired by the work of Cavicchi's group,[47,48] who modified natural rubber to possess shape memory behavior. In their work, rubber bands were swollen in molten stearic acid at 75 °C, which, upon cooling, resulted in materials with a permanent network derived from the rubber bands and a temporary network derived from the formation of microscopic stearic acid crystals across the rubber bands. The T_{trans} of the material was provided by the melting temperature of stearic acid at ∼70 °C, which gave shape memory performance with a reproducible 100% fixity and over 95% recovery. Cavicchi and co-workers[49] later demonstrated that the concentration of molten stearic acid solution (dissolved in isopropyl alcohol) correlated with the fixation of elastomeric foams, where higher concentrations resulted in better fixity in the foam. Since the materials in that work were porous, we hypothesized that the same chemistry would be effective in imparting shape memory behavior into polyHIPEs. In our work, we have synthesized porous SMP emulsion-templated polymers by premixing molten stearic acid with polysiloxanes in the continuous phase during the emulsification process before cross-linking. In our work, we have chosen to target materials with 65 and 30% total porosities; therefore, these fall under the classification of polyMIPEs. The incorporation of stearic acid into the polyMIPEs resulted in over 90% fixity and 95% recovery for up to 4 cycles of deformation. We anticipate that these PDMS-based SMPs will find uses in various technological fields such as soft robotics and deployable structures.

MATERIALS AND METHODS

Materials. The monomer 1,3,5-trivinyl-1,3,5-trimethylcyclotrisiloxane (TV_3) was purchased from AK Scientific (Union City, CA). Pyridine was purchased from Fisher Scientific (Hampton, NH). Chlorotrimethylsilane (TMSCl) was purchased from Oakwood Chemical (Estill, SC). The polymers [13−17% (mercaptopropyl) methylsiloxane]-dimethylsiloxane copolymer ("thiolated PDMS") (3500 g/mol), vinyl-terminated PDMS (vinyl-PDMS) (6000 g/mol), and (30−35% dodecylmethylsiloxane)-[7−10% hydroxy(propethyleneoxy (6−9) propyl) methylsiloxane] (55−65% dimethylsiloxane) terpolymer (Silube J208−812) were purchased from Gelest (Morrisville, PA). The photoinitiator 2,2-dimethoxy-2-phenylacetophenone (DMPA), reagent-grade dichloromethane (DCM), stearic acid, and the catalyst 1,5,7-triazobicyclo4.4.0dec-5-ene (TBD) were purchased from Sigma-Aldrich (St. Louis, MO). All of the reagents used in this work were used as received.

Methods. *Synthesis of Poly(methylvinylsiloxane) (PMVS).* Pendant vinyl siloxanes were synthesized using a modified procedure from the literature[50] with a ring-opening polymerization of cyclotrisiloxane initiated by water. In a representative synthesis, a 250 mL round-bottom flask was flame-dried and charged with a magnetic stir bar and septum. The flask was placed under a N_2 atmosphere while the monomer TV_3 and water were injected into the flask at a 15:1 molar ratio of monomer to water. A solution containing 0.15 mol equiv. of TBD with respect to water in (0.75 mL THF/gram of monomer) was then added to initiate the reaction and left to stir for 6 h at 30 °C. To halt the reaction and cap the polymer ends, pyridine (8 eq. with respect to water) and TMSCl (5 equiv) were added. Solvents were removed by bubbling N_2 through the reaction medium. The crude resin was washed three times with MeOH (75 mL) to yield a colorless oil (3.7 g, 61% mass recovery). The polymers were characterized using ^{1}H NMR and ^{13}C NMR spectroscopy (Figures S1 and S2) and gel permeation chromatography (GPC). ^{1}H NMR: (CDCl3, 400 MHz), 5.95 ppm (m, 2H), 5.8 ppm (dd 1H), 0.14 ppm (s, 3H). ^{13}C NMR: 136 ppm (s, CH2), 133 ppm (s, CH), −0.44 ppm (s, CH3). The PMVS samples used in this study were Mn ∼ 14,000 g/mol with $Đ$ = 1.15.

Preparation of MIPEs. In a typical experiment, silube (1.0 wt % w.r.t. polymers), thiolated PDMS (1.0 mol equiv), divinyl PDMS (0.5 mol equiv), PMVS (0.5 mol equiv), and stearic acid (28 wt % w.r.t. polymers) were added to a medium glass vial to produce the continuous phase of the emulsion template and heated to ∼80 °C until all of the stearic acid solids were melted. Water was emulsified into the vial containing siloxanes and stearic acid to produce either 30 or 65% volume fraction dispersed phases while keeping the vial hot with a heat gun and periodically vortexing the mixture. The emulsions were then photoinitiated by adding DMPA (5.0 wt % w.r.t. polymers) with a minimal (∼0.2 mL) amount of dichloromethane solvent.

PolyMIPE Synthesis. The emulsion templates were immediately exposed to UV radiation (λ = 365 nm) for 6 min without allowing the emulsion to cool. The cross-linked materials were removed from molds and allowed to dry at ambient conditions for 5−6 days until constant weight and then briefly rinsed in THF and set to dry until constant weight. The cross-linked polymer was analyzed using solid-state ^{13}C NMR without the inclusion of stearic acid to observe the disappearance of vinyl groups after the thiol−ene reaction in the continuous phase of the MIPEs (Figures S3 and S4).

Shape memory properties were quantified using cylinder-shaped samples cut to ∼6 to 7 mm height with ∼20 mm diameter. The samples were placed in boiling water for 1 h and then immediately removed and placed between 2 warm glass slides inside a circular mold of height ∼3 mm. The sample was then compressed between the slides to match the height of the circular mold at ∼3 mm. The slides were held with 2 office clamps, one on each side, and left at room temperature for 6 h. After this time, the samples were removed from the slides and left for 3 h at ambient conditions. Then, the samples were placed back into boiling water for 1 h, removed and dried, and their dimensions were measured using digital calipers. In each case, the height from the same face of each cylinder was used for measurement. The fixity and recovery were calculated with the following equations

$$F = (\varepsilon_f/\varepsilon_c) \times 100\% \quad (1)$$

$$R = (\varepsilon_f - \varepsilon_r)/(\varepsilon_f - \varepsilon_i) \times 100\% \quad (2)$$

where the initial strain (ε_i), compressed strain (ε_c), fixed strain (ε_f), and residual strain (ε_r) are obtained by

$$\varepsilon_x = (l_x - l_i)/l_i \quad (3)$$

where l_x is l_i, l_c, l_f, or l_r, having the same subscript as ε_x.

Total porosity was determined on dry polyMIPEs using an in-house Archimedes balance.[51] After calculating the measured density, the total porosity (Φ_{exp}) was calculated using eq 4

https://doi.org/10.1021/acs.macromol.4c00457
Macromolecules 2024, 57, 6796−6804

Scheme 1. Organocatalytic Ring-Opening Polymerization of Cyclotrisiloxane Initiated by Water for the Synthesis of Poly(methylvinylsiloxane)

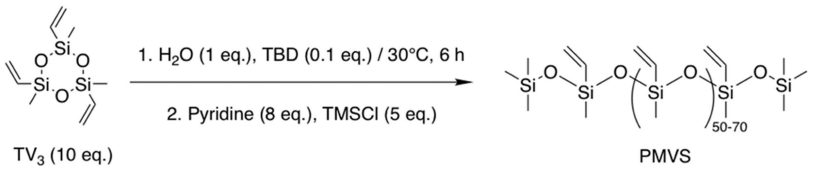

Scheme 2. Thiol−Ene Reaction in the Continuous Phase of the Emulsion Template Resulting in a Cross-Linked Network

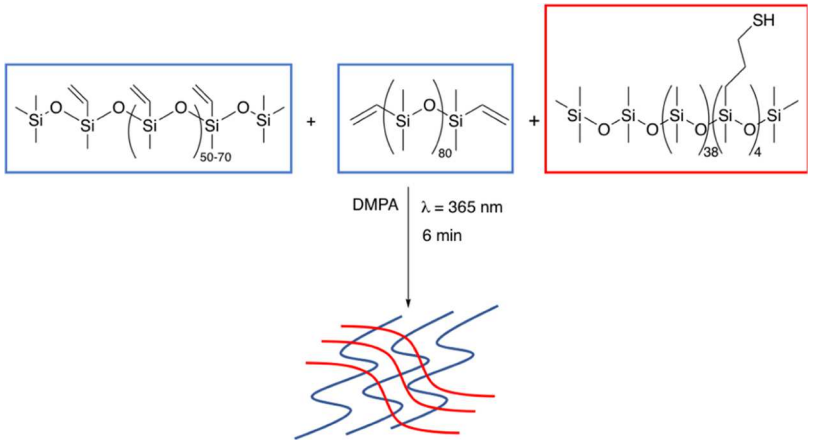

$$\Phi_{exp} = 1 - (\rho^*/\rho_0) \quad (4)$$

where ρ_0 is the average density of nonporous PDMS (0.975 g/mL) and ρ^* is the measured density of a polyMIPE sample. Fixity as a function of time was assessed for both porous and nonporous versions of these composites. Samples were fixed using the above procedure and left at ambient conditions. The fixity was measured at 2, 6, 18, and 36 h.

The recovery of the polyMIPEs was monitored as a function of temperature to characterize the transition temperature of the fixed network. Fresh polyMIPE cylinders were programmed by heating and then placing them in a circular mold between two glass slides as detailed above, and their lengths were recorded. The fixed polyMIPEs were then placed in water baths at set temperatures for 1 h. The length of the polyMIPE was then recorded again. The temperatures of the water baths were set from 60 to 85 °C in steps of 5 °C. The shape memory properties were demonstrated using either an oven or a heat gun to program and trigger shape memory properties. In these experiments, ∼65% total porosity materials were used following the same procedure outlined above except with alternative heating mechanisms (Figure S8, Tables S5 and S6).

^{1}H and ^{13}C{^{1}H} NMR spectra were collected on a Bruker AV 400, and the data were analyzed using MestreNova 14 software. Gel permeation chromatography (GPC) was performed to determine the molecular weight of PMVS using an Agilent 1200 series HPLC with filtered toluene (0.1% ethylbenzene w/v) eluent at a rate of 0.5 mL/min equipped with an Optilab rEX differential refractometer (light source 658 nm) detector calibrated against polystyrene standards and analyzed with ASTRA v. 6.1.0 software. The rheological behavior of the polyMIPEs was collected on a DHR-20 from TA Instruments operating in compression mode of up to 30% compression of the material. Young's moduli were obtained from the linear slope of the linear elastic region of each stress−strain curve from 0 to 10% strain. The pore morphology of polyMIPEs was imaged on a scanning electron microscope (SEM) (Low-Vac, FEI XL-30) equipped with an EDAX detector. Cross-sectional cuts of the material were placed on a copper wire and imaged at an accelerating voltage of 10 kV. Shear storage moduli were measured using a PerkinElmer dynamic mechanical analyzer (DMA-8000) and analyzed with Paris software. PolyMIPE samples were cut to ∼3 mm thick, ∼7 mm long, and ∼3 mm wide. Frequency sweeps were performed in a rectangular-tension geometry (0.1−70 Hz; 0.01 mm strain) on three separate samples for each type of material.

RESULTS

Our group has previously reported the synthesis of open-cell PDMS PolyHIPEs prepared using PMVS with sufficient cross-linking density to support high internal porosities.[51] In that work, PMVS was cross-linked with thiolated PDMS chains using UV light-photoinitiated thiol−ene Michael addition "click chemistry" reactions to produce polyHIPEs with total porosities of over 74%. In this work, we chose to use PMVS to provide a high compressibility for shape fixing during repeated cycles of deformations in SMP testing while avoiding bulk material damage. We synthesized PMVS according to Scheme 1.

We prepared the emulsion templates by dispersing an aqueous phase into the continuous phase consisting of stearic acid, polysiloxanes, and the DMPA photoinitiator with a small amount of dichloromethane (∼0.2 mL). Each emulsion was irradiated for 15 min, and the dispersed phase was removed by drying the polyMIPE at ambient conditions for 5−6 days until constant weight was achieved. The cross-linking reaction between polymers within the continuous phase is shown in Scheme 2.

We mixed the polysiloxanes with stearic acid in the emulsion template rather than dip-coating preprepared foams to prepare porous polymers with shape memory properties. We chose this route over dip-coating the polyMIPEs, as we observed a loss of internal porosity when immersing the prepared polyMIPEs into liquid stearic acid. For example, the total porosities of the polyMIPEs decreased from ∼60 to ∼20−30% following the inclusion of stearic acid into the preprepared porous materials. In contrast, melting the stearic acid into the polymers before emulsification maintained the templated internal porosity in the final materials. We prepared emulsion templates at two

https://doi.org/10.1021/acs.macromol.4c00457
Macromolecules 2024, 57, 6796−6804

different internal phase volume fractions. Lower total porosity (~30% porosity) samples were made from 30% internal phase volume fraction emulsions, while higher total porosity (~60% porosity) samples were made from emulsions containing an ~65% internal phase volume fraction. We anticipated that differences in the shape memory performance of these materials could occur as a result of the different pore sizes and pore wall morphologies anticipated at these two porosities. When we attempted to stabilize emulsions with internal phases higher than 65%, we observed complete phase separation of the emulsion due to the large amount of stearic acid disrupting emulsion stability. This is why, formally, only MIPEs and polyMIPEs are used in this work, and we did not prepare HIPE templates. We used 28 wt % stearic acid with respect to polymer weight of the siloxane prepolymers in these emulsions because the addition of more stearic acid caused the resulting materials to become extremely brittle. This loading of stearic acid is lower than that seen in the work from Cavicchi and coworkers[49] where a maximum loading of 43 wt % of stearic acid was used in polyurethane foams. However, in their work, a loading of ~5 wt % stearic acid was sufficient to observe shape memory behavior in their materials. The measured gel contents and total porosities of all of the porous materials prepared in this work are shown in Table 1.

Table 1. Measured Total Porosity and Weight of All PolyMIPE Samples

sample[a]	gel content[b] (%)	measured total porosity[c] (%, ±2)	Young's modulus (kPa)
low-porosity polyMIPE	96	30	4.0 ± 1.1
low-porosity polyMIPE + stearic acid	96	30	5.0 ± 2.75
high-porosity polyMIPE	96	62	0.6 ± 0.45
high-porosity polyMIPE + stearic acid	96	64	1.1 ± 0.87

[a]"Low" porosity refers to porous materials made using 30% dispersed phase volume templates, and "high" porosity refers to porous materials made using 65% dispersed phase volume templates. [b]Value calculated as the average from three samples. [c]Measured total porosity was calculated using three separate samples, with the water displacement method described in the Materials and Methods section.

We characterized the mechanical properties of the materials using a rheometer operating in a compression mode, and Young's moduli of the polyMIPEs were obtained from the linear slope of the linear elastic region of stress−strain curves up to 30% compression. Young's moduli values of the 30% porosity materials increase from ~4 kPa without stearic acid to ~5 kPa upon the inclusion of stearic acid, and the high-porosity materials possessing an ~60% total porosity are softer compared to the lower-porosity materials with Young's moduli of 0.6 kPa without stearic acid and 1.1 kPa with stearic acid. We suggest that the modest increase in Young's moduli in the materials with stearic acid compared to the analogous materials without stearic acid is a result of the crystalline stearic acid acting to reinforce the relatively soft polysiloxane-based network of the emulsion-templated materials. Thus, the polyMIPEs can be infused with stearic acid without becoming too hard and brittle to compress and expand.

We characterized the pore morphologies of the polyMIPEs with and without stearic acid using SEM imaging, and the results are shown in Figure 1. The materials prepared without stearic acid or heating the emulsion prior to polymerization are shown in Figure 1a,b, where Figure 1a is an image of the material from the 30% volume-dispersed phase emulsion template, and Figure 1b is the material from the 65% volume-dispersed phase emulsion template. The pore morphologies of the stearic acid composites are shown in the SEM images in Figure 1c,d, where Figure 1c is an image of the material from the 30% volume-dispersed phase emulsion template, and Figure 1d is the material from the 65% volume-dispersed phase emulsion template.

It can be seen in Figure 1 that while the control samples have defined pore diameters of around 8−9 mm for the lower-porosity materials and approximately 5−6 mm for the higher-porosity materials, the stearic acid composites have nonuniform voids with end-to-end distances >100 mm. The porous polymers without stearic acid have spherical-shaped pores, while the materials containing stearic acid do not have a defined pore wall shape. We confirmed that the change in pore morphology is due to the presence of the stearic acid in the template rather than the heating in the synthesis protocol by preparing control samples with no stearic acid but using the same heating steps. The pore morphologies of these heated controls (Figure S5a,b) were identical to the materials prepared without heating (Figure S6a,b). However, there are noticeable differences in the pore morphologies of the materials prepared with stearic acid and those materials without. The addition of stearic acid causes the continuous phase of the emulsion template to behave differently compared to without the stearic acid. This may potentially be as a result of the hydrophilic carboxylic acid groups in stearic acid disrupting the aqueous droplets in the dispersed phase of the emulsion. Alternatively, the stearic acid may act as a cosurfactant in the emulsion template.

The polyMIPE shape memory behavior was evaluated by fixing the materials in a compressed shape. First, materials of ~6 mm height were submerged in boiling water for an hour and then removed and placed between two glass slides. The slides were compressed to ~3 mm and held for 6 h at ambient conditions. After this time, the height of the cylinder was recorded. Glass slides were subsequently removed and the fixed polyMIPEs were left at ambient conditions for 3 h and their height was measured again. The programmed polyMIPEs were then submerged in boiling water for an hour to recover their initial shape, and their heights were measured a final time. This process was repeated in 3 more cycles. The visual appearance of a polyMIPE and its fixed analogue is provided in Figure 2. After each recovery, the samples were placed under compression rheology tests to determine their Young's moduli. This was done to elucidate whether or not the material's structural integrity was being damaged during compressive programming of a temporary shape.

We also prepared control polyMIPEs to demonstrate the effect of the stearic acid on SMP behavior. One control was prepared without stearic acid, and a second was prepared without stearic acid but still heating the emulsion. Neither of these polyMIPEs exhibited shape memory properties, confirming that the observed shape memory behavior of our materials is a result of the stearic acid within the PDMS-based networks.

We examined the SMP polyMIPEs using SEM imaging after fixation to observe the pore morphology changes under compression. SEM images of the fixed polyMIPEs are shown in Figure 3.

https://doi.org/10.1021/acs.macromol.4c00457
Macromolecules 2024, 57, 6796−6804

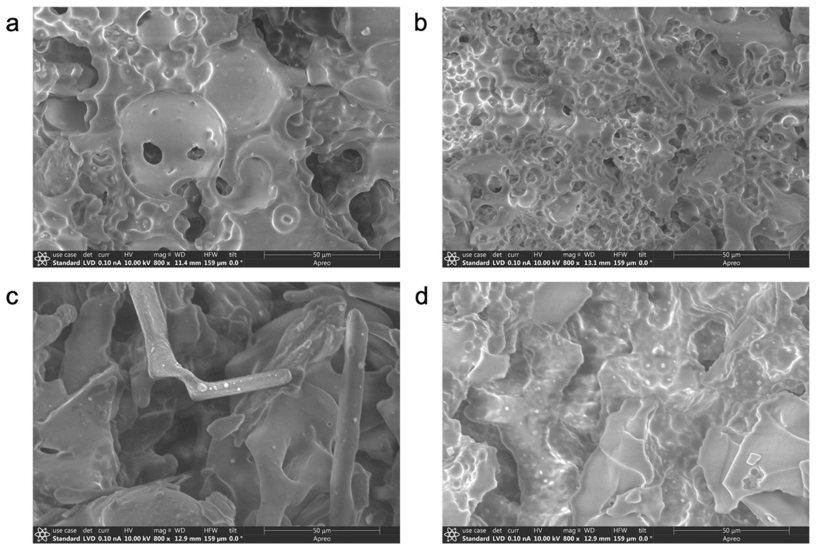

Figure 1. SEM images showing the pore morphology of (a) 31% porosity polyMIPE with no stearic acid; (b) 61% porosity polyMIPE with no stearic acid; (c) 30% porosity polyMIPE with stearic acid; and (d) 64% porosity polyMIPE with stearic acid. The scale bar in the images is 50 μm.

Figure 2. Image showing the appearance of (left to right) fixed polyMIPE, recovered polyMIPE, and thumbtack for size reference.

When comparing the fixed morphologies from Figure 3 with their noncompressed analogues in Figure 1c,d, it appears that the pores remain intact, which suggests that compressing the materials to 70% did not result in either a collapse of the internal porosity or widespread damage of the material.

We quantified the shape memory properties of the emulsion-templated materials over four cycles of fixing and recovery using shape fixity and recovery calculations from measurements of the polyMIPE dimensions in their temporary and permanent shapes.

The fixity values for both low- and high-porosity samples were above 90% throughout each cycle where higher-porosity samples have a slightly higher fixity (Figure 4). We suggest that the higher fixity values in the more porous samples are a result of these materials containing more void space, which allows for easier deformation to the material and less propensity to push back against deformation.

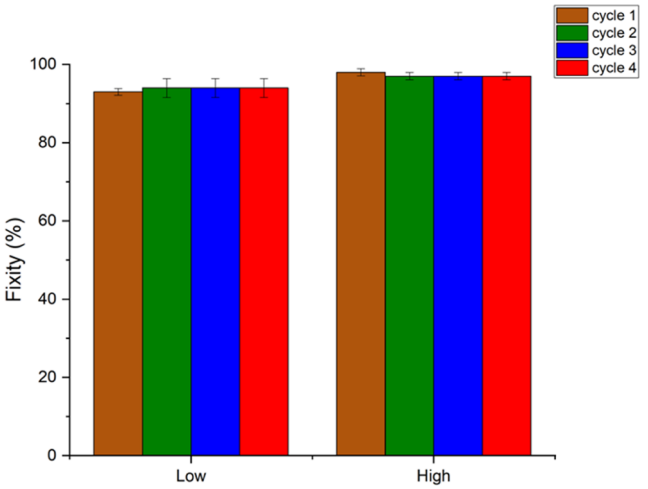

Figure 4. Fixity values in 4 subsequent cycles for PMVS/SA polyMIPEs with low (~30%) and high (~60%) total porosities. Data is averaged over three samples at each formulation.

It is known that in some SMPs the fixity of the material can be seen to reduce over time, often due to creep relaxation in the polymer reducing the number of effective cross-links caused by chain entanglements.[52,53] For example, in previous work from our group on glucose-functionalized polyurethane/urea, we observed a fast relaxation within the first 30 h after

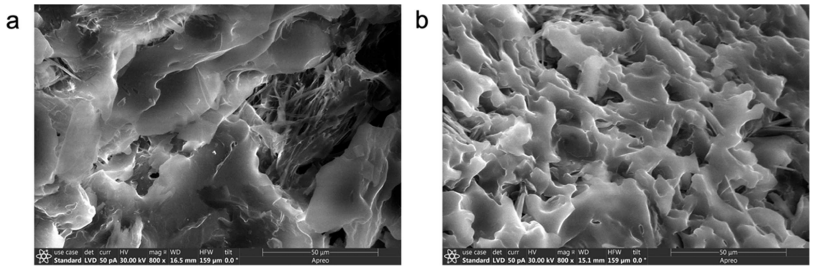

Figure 3. SEM images showing the pore morphology of polyMIPEs under shape fixation while compressed to ~70% volume. (a) 30% porosity polyMIPE and (b) 61% porosity. The scale bar in the images is 50 μm. (Images taken under the first cycle of fixity).

https://doi.org/10.1021/acs.macromol.4c00457
Macromolecules 2024, 57, 6796−6804

fixation due to a decrease in residual stress on polymer chains that naturally occurs over time.[54] To observe if a similar effect was occurring in these polysiloxane/stearic acid blends, we fixed materials on the first cycle and allowed them to rest at ambient conditions for over 36 h while periodically measuring their fixity score. The results from this experiment are shown in Figure 5.

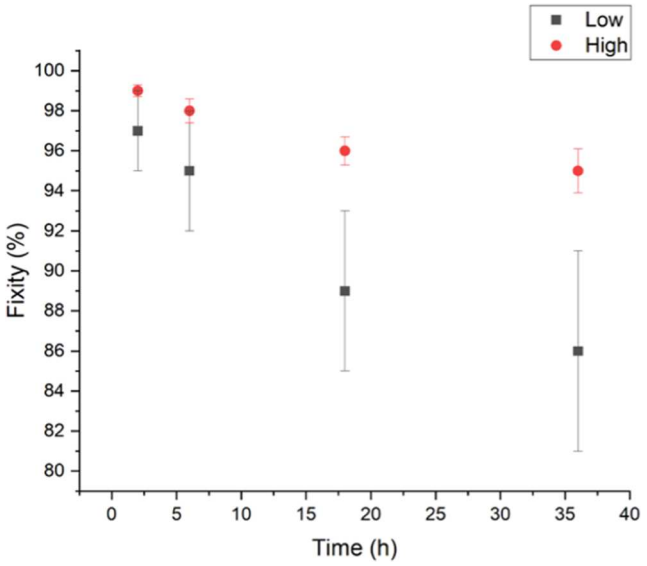

Figure 5. Average fixity as a function of time for low-porosity (30, 30, and 31%) and high-porosity (65, 63, and 60%) PMVS/SA polyMIPE samples.

While we observed only small differences between high- vs low-porosity materials with respect to initial fixity, when we observed the fixity as a function of time, we saw different behaviors in the two materials. Overall, the fixity remained above 84% in the low-porosity samples, whereas the fixity remained above 93% in the high-porosity samples. The fixity values decreased over the first 24 h due to a fast strain relaxation of polymer chains followed by fixity values approaching a plateau at 36 h. This is similar to the behavior observed in our prior work on porous polyurethane materials.[54] Interestingly, the high-porosity materials maintained a higher fixity score over time compared to the lower-porosity materials. We attribute this behavior to the smaller regions of polysiloxane between the pores in the ∼60% porosity materials (i.e., the different pore morphologies). We further tested the shape memory properties of the polysiloxane/stearic acid matrix in a nonporous material and observed similar behavior of deformation recovery over time. Qualitative images showing the loss in fixity over 36 h are depicted in Figure S7. Compared to the porous polyMIPE materials, the nonporous analogues tend to break under more than one cycle of deformation.

The shape change of the polyMIPEs was measured as a function of temperature (Figure 6) by fixing the materials and then placing the materials into different water baths from set at 60−85 °C in steps of 5 °C and measuring their recovery response. We observed a sharp change in shape in the materials from 65 to 70 °C, which we suggest is due to the melting point of stearic acid and the materials being porous.

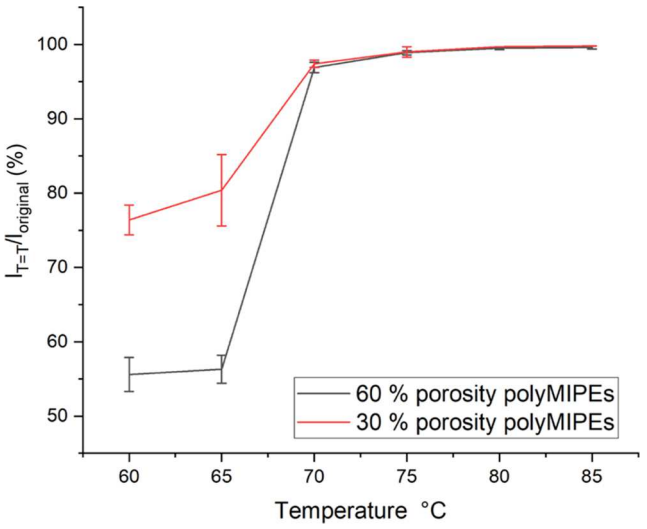

Figure 6. Changes in shape as temperature is increased from 60 to 85 °C. In the *y*-axis, $l_{T=T}$ is the length of the material at the temperature of the observation and $l_{original}$ is the original length of the material before fixing.

The recovery of all polyMIPEs was above 95%, but the higher total porosity samples had slightly higher recovery (Figure 7).

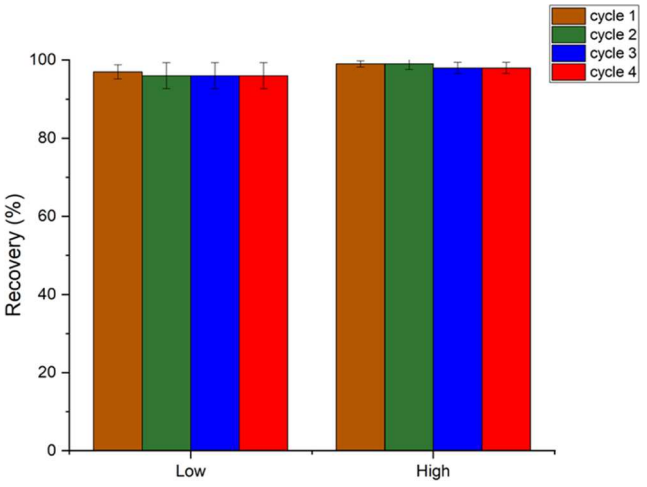

Figure 7. Recovery values in 4 subsequent cycles for PMVS/SA polyMIPEs with low and high total porosities. (Low refers to materials possessing an internal total porosity of ∼30%. High refers to those with ∼60%).

All trends in shape memory behavior were consistent throughout four cycles of compression on the polyMIPEs, suggesting that these materials can be recycled multiple times. We expected the recovery of the materials to be relatively high and similar to each other due to the elastic nature of PDMS. Furthermore, we have demonstrated that the shape fixing and recovery of these PDMS-based polyMIPEs can be achieved using alternative heating methods to immersion in hot water. Specifically, we have used both a temperature-programmed oven and a heat gun to provide rapid heating. The results from these experiments can be found in Table S6, and images of the shape memory cycles are presented in Figure S8.

We monitored Young's moduli of samples after each recovery cycle from the water-heating method to ensure that

https://doi.org/10.1021/acs.macromol.4c00457
Macromolecules 2024, 57, 6796−6804

compressive programming was not damaging the material (Figure 8).

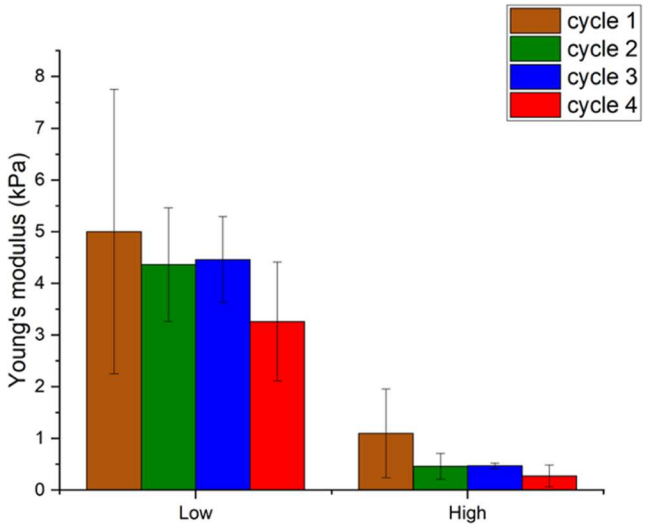

Figure 8. Young's modulus of low- and high-porosity PMVS/SA polyMIPEs throughout shape memory cycles 1−4. (Low refers to materials possessing an internal total porosity of ∼30%. High refers to those with ∼60%).

Young's moduli values decreased following each recovery cycle in absolute values, although they remained statistically consistent, suggesting no widespread breakage during compressive deformation. We determined that the polyMIPEs lost between 1 and 4% mass after the first heating process, and we speculate that this could be a cause of the reduction in the absolute value of Young's modulus observed We confirmed the insignificance in the change in Young's modulus by performing *t* tests on the data at 95% confidence interval, and no *t*-value was higher than the *p*-value (Table S1). This result suggests that these materials are resilient enough to be heated and compressed repeatedly, at least over four cycles, without breaking. We believe that the difference in shape memory behavior and resiliency between the nonporous materials and these polyMIPEs is a consequence of the polyMIPE porosity. Due to the porous nature of the polyMIPEs, these materials are fixed using compression as opposed to the twisting or extension used in the nonporous materials. We believe that the lower moduli of porous materials compared to analogous nonporous materials (see Figure S9 and Table S7 for the storage moduli of samples used in this work) result in easier recovery of the permanent shape for the polyMIPEs.

CONCLUSIONS

A shape memory polyMIPE was successfully prepared by mixing molten stearic acid into the emulsion-templated precursor. To the best of our knowledge, this is the first example of a PDMS polyMIPE capable of shape memory properties, achieving fixity scores over 90% and recovery ratios over 95% across multiple deformation cycles. By SEM imaging, we confirm the drastic change in pore morphology when molten stearic acid is added to the emulsion template. Higher porosities yielded slightly improved shape memory performance initially but significantly improved performance over time. Both samples (high and low porosities) exhibited a reduction in the materials Young's moduli upon each recovery cycle. We anticipate that this chemistry can apply to several soft polymers, which may broadly impact the design of new shape memory polyHIPEs, and we envision that these materials can be used in soft robotics and biomimetic materials.

ASSOCIATED CONTENT

Supporting Information

The Supporting Information is available free of charge at https://pubs.acs.org/doi/10.1021/acs.macromol.4c00457.

Molecular weight characterization, NMR, control emulsions, qualitative loss in fixity over time, and *t* test results (PDF)

AUTHOR INFORMATION

Corresponding Author

Neil Ayres − *Department of Chemistry, The University of Cincinnati, Cincinnati, Ohio 45221, United States;* orcid.org/0000-0001-8718-2502; Phone: +01 513 556 9280; Email: neil.ayres@uc.edu; Fax: +01 513 556 9239

Authors

Anthony Smith − *Department of Chemistry, The University of Cincinnati, Cincinnati, Ohio 45221, United States*

Anna Brown − *Department of Chemistry, The University of Cincinnati, Cincinnati, Ohio 45221, United States*

Jack Newman − *Department of Chemistry, The University of Cincinnati, Cincinnati, Ohio 45221, United States*

Complete contact information is available at: https://pubs.acs.org/10.1021/acs.macromol.4c00457

Author Contributions

The manuscript was written through contributions of all authors. All authors have given approval to the final version of the manuscript.

Notes

The authors declare no competing financial interest.

ACKNOWLEDGMENTS

The authors thank the National Science Foundation (DMR-1940518) for the resources to complete this study.

REFERENCES

(1) Lendlein, A.; Kelch, S. Shape-memory Polymers. *Angew. Chem.* **2002**, *41* (12), 2034−2057.

(2) Lendlein, A.; Jiang, H.; Juenger, O.; Langer, R. Light-induced Shape Memory Polymers. *Nature* **2005**, *434*, 879−882.

(3) Small, W., IV; Singhal, P.; Wilson, T.; Maitland, D. Biomedical Applications of Thermally Activated Shape Memory Polymers. *J. Mater. Chem.* **2010**, *20*, 3356−3366.

(4) Woodard, L.; Kmetz, K.; Roth, A.; Page, V.; Grunlan, M. Porous Poly(E-caprolactone)-poly(L-lactic acid) Semi Interpenetrating Networks as Superior, Defect Specific Scaffolds with Potential for Cranial Defect Repair. *Biomacromolecules* **2017**, *18* (12), 4075−4083.

(5) Heuwers, B.; Quintmann, D.; Katzenberg, F.; Tiller, J. Stress-induced Melting of Crystals in Natural Rubber: A New Way to Tailor the Transition Temperature of Shape Memory Polymers. *Macromol. Rapid Commun.* **2012**, *33* (18), 1517−1522.

(6) Charlesby, A. *Atomic Radiation and Polymers*; Pergamon Press: Oxford, 1960; pp 198−257.

(7) Machi, S. New Trends of Radiation Processing Applications. *Radiat. Phys. Chem.* **1996**, *47*, 333−336.

(8) Lendlein, A.; Langer, R. Biodegradable, Elastic, Shape-memory Polymers for Potential Biomedical Applications. *Science* **2002**, *296*, No. 5573.
(9) Yakacki, C. M.; Shandas, R.; Lanning, C.; Bech, B.; Eckstein, A.; Gall, K. Unconstrained Recovery Characterization of Shape-memory Polymer Networks for Cardiovascular Applications. *Biomaterials* **2007**, *28* (14), 2255−2263.
(10) Peng, Q.; Wei, H.; Qin, Y.; Yuyang, L.; Zaishan, Z.; Zhao, X.; Xu, F.; Leng, J.; He, H.; Cao, A.; Li, Y. Shape Memory Polymer Nanocomposites with a 3D Conductive Network for Bidirectional Actuation and Locomotion Application. *Nanoscale* **2016**, *8* (42), 18042−18049.
(11) Ishida, K.; Hortensius, R.; Luo, X.; Mather, P. Soft Bacterial Polyester-based Shape Memory Nanocomposites Featuring Reconfigurable Nanostructure. *J. Polym. Sci., Part B: Polym. Phys.* **2012**, *50* (6), 387−393.
(12) Li, Z.; Hu, J.; Ma, L.; Liu, H. High Glass-transition Temperature Shape-memory Materials: Hydroxyl-terminated Polydimethylsiloxane-modified Cyanate Ester. *J. Appl. Polym. Sci.* **2020**, *137* (18), No. 48641.
(13) Kai, D.; Tan, M.; Prabhakaran, M.; Chan, B.; Liow, S.; Ramakrishna, S.; Loh, X. Biocompatible Electrically Conductive Nanofibers from Inorganic-organic Shape Memory Polymers. *Colloids Surf., B* **2016**, *148*, 557−565.
(14) Schmidt, A. M. Electromagnetic Activation of Shape Memory Polymer Networks Containing Magnetic Nanoparticles. *Macromol. Rapid Commun.* **2006**, *27* (14), 1168−1172.
(15) Kim, Y.-J.; Matsunaga, Y. Thermo-responsive Polymers and their Application as Smart Biomaterials. *J. Mater. Chem. B* **2017**, *5* (23), 4307−4321.
(16) Chen, M.-C.; Tsai, H. W.; Tsia, H.; Chang, Y.; Lai, W.; Mi, F.; Liu, C.; Wong, H. S. Rapidly Self-expandable Polymeric Stents with a Shape-memory Property. *Biomacromolecules* **2007**, *8* (9), 2774−2780.
(17) Huang, W. M.; Yang, B.; Zhao, Y.; Ding, Z. Thermo-moisture Responsive Polyurethane Shape-memory Polymer and Composites: a review. *J. Mater. Chem.* **2010**, *20*, 3367−3381.
(18) Liu, Y.; Li, Y.; Yang, G.; Zheng, X.; Zhou, S. Multi-stimulus-responsive Shape-memory Nanocomposite Network Cross-linked by Cellulose Nanocrystals. *ACS Appl. Mater. Interfaces* **2015**, *5*, 4307−4321.
(19) Tay, R. Y.; Li, H.; Lin, J.; Wang, H.; Lim, J.; Chen, S.; Leong, W.; Tsang, E. T.; Teo, E. H. T. Lightweight, Superelastic Boron Nitride/polydimethylsiloxane Foam as Air Dielectric Substitute for Multifunctional Capacitive Sensor Applications. *Adv. Funct. Mater.* **2020**, *30* (10), No. 1909604.
(20) Mason, I.; Guy, S.; Sage, I.; Mcdonnell, D.; Cameron, N.; Sherrington, D. A Switchable Liquid Crystal Impregnated Porous Polymer Device. *Mol. Cryst. Liq. Cryst. Sci. Technol., Sect. A* **1995**, *263*, 2499−2507.
(21) Fu, X.; Wang, P.; Miao, Q.; Liu, K.; Liu, H.; Liu, J.; Fang, Y. Polymerizable Organo-gelator-stabilized gel-emulsions toward the Preparation of Compressible Porous Polymeric Monoliths. *J. Mater. Chem. A* **2016**, *4* (39), 15215−15223.
(22) Kumar, R.; Jin, Y.; Marre, S.; Poncelet, O.; Brunet, T.; Leng, J.; Mondain-Monval, O. Drying Kinetics and Acoustic Properties of Soft Porous Polymer Materials. *J. Porous Mater.* **2021**, *28* (1), 249−259.
(23) McKenzie, T. J.; Rost, K.; Smail, S.; Mondain-Monval, O.; Brunet, T.; Ayres, N. Mechanically Tunable PDMS-based PolyHIPE Acoustic Materials. *J. Mater. Chem. C* **2022**, *10*, 6222−6226.
(24) Peng, Y.; Li, Q.; Seekell, R.; Kheir, J.; Porter, B.; Polizzotti, B. Tunable Nonlinear Acoustic Reporters Using Micro- and Nanosized Air Bubbles with Porous Polymeric Hard Shells. *ACS Appl. Mater. Interfaces* **2019**, *11* (1), 7−12.
(25) Kovalenko, A.; Fauqignon, M.; Brunet, T.; Mondain-Monval, O. Tuning the Sound Speed in Microporous Polymers with a Hard or Soft Matrix. *Soft Matter* **2017**, *13* (25), 4526−4532.
(26) Kovalenko, A.; Zimny, K.; Mascaro, B.; Brunet, T.; Mondain-Monval, O. Tailoring of the Porous Structure of Soft Emulsion Templated Materials. *Soft Matter* **2016**, *12* (23), 5154−5163.
(27) Tripp, J. A.; Stein, J.; Svec, F.; Fréchet, J. "Reactive Filtration": Use of Functionalized Porous Polymer Monoliths as Scavengers in Solution-phase Synthesis. *Org. Lett.* **2000**, *2* (2), 195−198.
(28) Robinson, J. L.; Moglia, R.; Steubben, M.; Mcenery, M.; Cosgriff-Hernandez, E. Achieving Interconnected Pore Architecture in Injectable PolyHIPEs for Bone Tissue Engineering. *Tissue Eng., Part A* **2014**, *20* (5−6), 1102−1112.
(29) Shea, L. D.; Wang, D.; Franceschi, R.; Mooney, D. Engineered Bone Development from a Pre-Osteoblast Cell Line on Three-dimensional Scaffolds. *Tissue Eng.* **2000**, *6* (6), 605−617.
(30) Wu, D.; Xu, F.; Sun, B.; Fu, R.; He, H.; Matyjaszewski, K. Design and Preparation of Porous Polymers. *Chem. Rev.* **2012**, *112* (7), 3959−4015.
(31) Silverstein, M. S. PolyHIPEs: Recent Advances in Emulsion-templated Porous Polymers. *Prog. Polym. Sci.* **2014**, *39* (1), 199−234.
(32) Silverstein, M. S. Emulsion-templated Porous Polymers: A Retrospective Perspective. *Polymer* **2014**, *55* (1), 304−320.
(33) Xu, T.; Li, G. A Shape Memory Polymer Based Syntactic Foam with Negative Poisson's Ratio. *Mater. Sci. Eng. A* **2011**, *528* (22−3), 6804−6811.
(34) Ahn, J.-S.; Yu, W.; Youk, J.; Ryu, H. In situ Temperature Tunable Pores of Shape Memory Polyurethane Membranes. *Smart Mater. Struct.* **2011**, *20*, No. 105024.
(35) Zhang, D.; Burkes, W.; Schoener, C.; Grunlan, M. Porous Inorganic-organic Shape Memory Polymers. *Polymer* **2012**, *53* (14), 2935−2941.
(36) Tobushi, H.; Okumura, K.; Endo, M.; Hayashi, S. Thermomechanical Properties of Polyurethane-shape Memory Polymer Foam. *J. Intell. Mater. Syst. Struct.* **2001**, *12* (4), 283−287.
(37) Livshin, S.; Silverstein, M. Crystallinity in Cross-linked Porous Polymers from High Internal Phase Emulsions. *Macromolecules* **2007**, *40* (17), 6349−6354.
(38) Ang, J. Y.; Chan, B.; Kai, D.; Loh, X. Engineering Porous Water-Responsive poly(PEG/PCL/PDMS urethane) Shape Memory Polymers. *Macromol. Mater. Eng.* **2017**, *302* (9), No. 1700174.
(39) Zhang, T.; Sanguramath, S.; Israel, S.; Silverstein, M. Emulsion Templating: Porous Polymers and Beyond. *Macromolecules* **2019**, *52* (15), 5445−5479.
(40) Kim, K. S.; Zhao, Y.; Jang, H.; Lee, S.; Kim, J.; Kim, K.; Ahn, J.; Kim, P.; Choi, J.; Hong, B. Large-scale Pattern Growth of Graphene Films for Stretchable Transparent Electrodes. *Nature* **2009**, *457*, 706−710.
(41) Zhao, Y.-H.; Zhang, Y.; Bai, S. High Thermal Conductivity of Flexible Polymer Composites Due to Synergistic Effect of Multilayer Graphene Flakes and Graphene Foam. *Composites, Part A* **2016**, *85*, 148−155.
(42) Hu, J.; Ly, G.; Ning, N.; Yu, B.; Tian, M.; Zhang, L. Comfort Fitting Shape Memory Elastomer with Constructed Strong Interface based on Amphiphilic Hybrid Janus Particles. *Composites, Part B* **2022**, *236*, No. 109828.
(43) Schoener, C. A.; Weyand, C.; Murthy, R.; Grunaln, M. Shape Memory Polymers with Silicon-containing Segments. *J. Mater. Chem.* **2010**, *20* (9), 1787−1793.
(44) Chan, B. Q. Y.; Heng, S.; Liow, S.; Zhang, K.; Loh, X. Dual-responsive Hybrid Thermoplastic Shape Memory Polyurethane. *Mater. Chem. Front.* **2017**, *1*, 767−779.
(45) Rao, Y.-L.; Chortos, A.; Pfattner, R.; Lissel, F.; Chiu, Y. C.; Feig, V.; Xu, J.; Kurusawa, T.; Gu, X.; Wang, C.; He, M.; Chung, J.; Bao, Z. Stretchable Self-healing Polymeric Dielectrics Cross-linked Through Metal-ligand Coordination. *J. Am. Chem. Soc.* **2016**, *138* (18), 6020−6027.
(46) Gossweiler, G. R.; Hewage, G.; Soriano, G.; Wang, Q.; Welshofer, G.; Zhao, X.; Craig, S. Mechanochemical Activation of Covalent Bonds in Polymers with Full and Repeatable Macroscopic Shape Recovery. *ACS Macro Lett.* **2014**, *3* (3), 216−219.
(47) Brostowitz, N. R.; Weiss, R.; Cavicchi, K. Facile Fabrication of a Shape Memory Polymer by Swelling Cross-linked Natural Rubber with Stearic Acid. *ACS Macro Lett.* **2014**, *3* (4), 374−377.

https://doi.org/10.1021/acs.macromol.4c00457
Macromolecules 2024, 57, 6796−6804

(48) Pantoja, M.; Lin, Z.; Cakmak, M.; Cavicchi, K. Structure-property Relationships of Fatty Acid Swollen, Crosslinked Natural Rubber Shape Memory Polymers. *J. Polym. Sci., Part B: Polym. Phys.* **2018**, *56* (8), 673−688.
(49) Pantoja, M.; Alvarado, T.; Cakmak, M.; Cavicchi, K. Stearic Acid Infused Polyurethane Shape Memory Polymer Foams. *Polymer* **2018**, *153*, 131−138.
(50) Fuchise, K.; Igarashi, M.; Sato, K.; Shimada, S. Organocatalytic Controlled/living Ring-opening Polymerization of Cyclotrisiloxanes Initiated by Water with Strong Organic Base Catalysts. *Chem. Sci.* **2018**, *9* (11), 2879−2891.
(51) Smith, A.; Ayres, N. Open-cell PDMS PolyHIPEs Prepared using Polymethylvinylsiloxane to Prevent Pore Collapse. *Polymer* **2023**, *270*, No. 125787.
(52) Hutchinson, J. M.; Cortes, P. Physical Aging of Shape Memory Polymers Based upon epoxy-thiol "click" Systems. *Polym. Test.* **2018**, *65*, 480−490.
(53) Hao, J.; Weiss, R. Mechanically Tough, Thermally Activated Shape Memory Hydrogels. *ACS Macro Lett.* **2013**, *2* (1), 86−89.
(54) Chai, Q.; Huang, Y.; Ayres, N. Shape Memory Biomaterials Prepared from Polyurethane/ureas Containing Sulfated Glucose. *J. Polym. Sci., Part A: Polym. Chem.* **2015**, *53* (19), 2252−2257.

https://doi.org/10.1021/acs.macromol.4c00457
Macromolecules 2024, 57, 6796−6804